ISBN: 978-3-95450-201-1 doi:10.18429/JACoW-IBIC2018-WEPB11

SPATIAL RESOLUTION IMPROVEMENT OF OTR MONITORS BY OFF-AXIS LIGHT COLLECTION

A. Potylitsyn[1,†], L. Sukhikh[1], G. Kube[2], A. Novokshonov[1,2]
[1]Tomsk Polytechnic University, 30, Lenin St., Tomsk, 634050, Russia
[2] Deutsches Elektronen-Synchrotron (DESY), Hamburg, Germany

Abstract

The spatial resolution of an OTR monitor, widely used for electron beam profile diagnostics, is determined by the resolution of the optical system and by the Point Spread Function (PSF) representing the single electron image. In the image plane, the PSF has a typical lobe-shape distribution with an inter-peak distance depending on wavelength and lens aperture ratio [1]. For a beam with a transverse rms size smaller than the distance, the reconstruction of the beam profile has several difficulties [2, 3]. We propose to reduce the PSF contribution and to improve the spatial resolution of an OTR monitor simply by rotating the lens optical axis with respect to the specular reflection direction. If the difference between the rotational angle and the lens aperture is much larger than the inverse Lorentz factor, the PSF has a Gaussian-like distribution which matches practically with the Airy distribution. Thus the resolution depends on wavelength and lens aperture. In principle, for lens apertures in the order of 0.1 rad such an approach should allow to measure beam sizes comparable to the wavelength of observation, using a simple deconvolution procedure for the measured image and the PSF.

INTRODUCTION

Transverse beam size measurements based on optical transition radiation (OTR) are a widely used technique and OTR monitor stations are operated at most modern electron linacs [4, 5]. For electron energies higher than 50 MeV the OTR intensity collected by a conventional optics system with numerical aperture of $\theta_m \sim 0.1$ rad achieves $N_{ph} \sim 10^{-3}$ photons per electron in the band width $\Delta\lambda / \lambda \sim 0.05$.

The spatial resolution of a transverse beam size monitor based on OTR is determined by the so-called Point Spread Function (PSF) or, in other words, by the response of the monitor optical system to a point charge crossing the target. With knowledge of the PSF, in principle it is possible to reconstruct beam size and beam shape from an electron bunch passing through the target applying a deconvolution algorithm to the measured OTR image.

The PSF has a double-lobe structure which is defined by the radiation wavelength λ, the acceptance angle or numerical aperture of the optical system θ_m, and the alignment accuracy. For the condition of ideal imaging the OTR monitor resolution determined by so-called diffraction limit can be expressed as

$$R = 1{,}12\frac{\lambda M}{\theta_m}. \tag{1}$$

Here M denotes the magnification factor of the optical system.

For beams with micrometer/submicrometer sizes such an optical system provides PSF dominated regime and one should applicate a spectral treatment of the data in order to extract a real beam size [6].

We propose optical schemes for OTR monitors with off-axis light collection in order to avoid a two-lobe structure of the PSF and improve its spatial resolution.

CALCULATIONS OF OTR PSF DISTRIBUTIONS

Under ultra-relativistic approximation the particle Coulomb field can be sufficiently described by its transverse components and it is possible to write down the OTR field in the lens plane in analogy with wave scattering at a finite size conducting screen:

$$E^L_{x,y}(\mathrm{X}_L,\mathrm{Y}_L) = \mathrm{const}\int_{S_T} d\mathrm{X}_T d\mathrm{Y}_T \begin{Bmatrix}\cos\varphi_T \\ \sin\varphi_T\end{Bmatrix} K_1\left(\frac{k}{\beta\gamma}R_T\right)\times$$
$$\exp\left[i\frac{k}{2a}\left(\mathrm{X}_T^2+\mathrm{Y}_T^2\right)\right]\exp\left[-i\frac{k}{a}\left(\mathrm{X}_L\mathrm{X}_T+\mathrm{Y}_T\mathrm{Y}_L\right)\right]. \tag{2}$$

Here $R_T = \sqrt{\mathrm{X}_T^2+\mathrm{Y}_T^2}$, ($\mathrm{X}_T$, Y_T) and ($\mathrm{X}_L,\mathrm{Y}_L$) are the coordinates of target surface and lens plane, a is the distance between target and lens, S_T is the target surface area, $\begin{Bmatrix}\cos\varphi_T \\ \sin\varphi_T\end{Bmatrix} = \frac{1}{\sqrt{\mathrm{X}_T^2+\mathrm{Y}_T^2}}\begin{Bmatrix}\mathrm{X}_T \\ \mathrm{Y}_T\end{Bmatrix}$, $K_1(x)$ is the MacDonald function of the first order, $k = 2\pi/\lambda$.

The OTR fields in the image plane using thin lens approximation can be written in the following way after integration over the lens aperture S_L:

$$E^D_{x,y}(\mathrm{X}_D,\mathrm{Y}_D) = \mathrm{const}\int_{S_L} d\mathrm{X}_L d\mathrm{Y}_L E^L_{X,Y}(\mathrm{X}_L,\mathrm{Y}_L)\times$$
$$\exp\left[-i\frac{k}{b}\left(\mathrm{X}_L\mathrm{X}_D+\mathrm{Y}_L\mathrm{Y}_D\right)\right]. \tag{3}$$

b is the distance between lens and detector. Inserting Eq. (2) in the last expression and performing 4-fold

† email: potylitsyn@tpu.ru

Content from this work may be used under the terms of the CC BY 3.0 licence (© 2018). Any distribution of this work must maintain attribution to the author(s), title of the work, publisher, and DOI.

ISBN: 978-3-95450-201-1 doi:10.18429/JACoW-IBIC2018-WEPB11

Content from this work may be used under the terms of the CC BY 3.0 licence (© 2018). Any distribution of this work must maintain attribution to the author(s), title of the work, publisher, and DOI.

integration, one can obtain the OTR fields and, subsequently, PSF distribution [7, 8]:

$$\frac{d^2W}{\hbar d\omega d\Omega} = \text{const}\left(\left|E_x^D\right|^2 + \left|E_y^D\right|^2\right) = \text{const}\left(\frac{d^2W_x^D}{\hbar d\omega d\Omega} + \frac{d^2W_y^D}{\hbar d\omega d\Omega}\right). \tag{4}$$

Figure 1 shows PSF distributions calculated for the following parameters: $\lambda = 0.5$ um; $\gamma = 2000$; $a = b = 500$ mm; the lens diameter $d_L = 100$ mm (green curve) and $d_L = 50$ mm (blue curve).

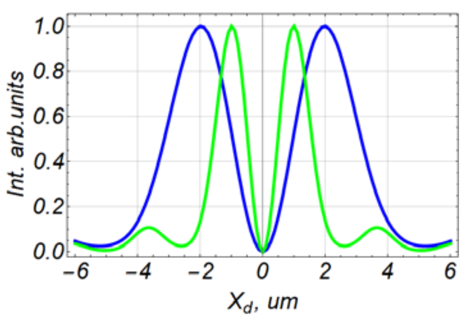

Figure 1: PSF distributions for horizontal polarization component $d^2W_x^D / \hbar d\omega d\Omega$ for $y_D = 0$.

METHODS FOR IMPROVEMENT OF THE OTR SPATIAL RESOLUTION

Basis of the first method is the installation of a mask in front of the lens with appropriate size at a position which is asymmetric with respect to the optical axis. If mask size and position are selected in a proper way it is possible to block one of the lobes of the horizontal angular OTR distribution. In this case information is extracted only from the second lobe in the lens plane or in the $k_x - k_y$ phase space. Due to the properties of the Fourier transformation the output in the $X_D - Y_D$ plane (i.e. the detector plane) will also have a single maximum distribution.

For such asymmetric geometry the PSF distribution can be calculated from the above mentioned expressions (1)–(3) with integration in (2) over the open part of the lens (Fig. 2).

The single maximum PSF in this case can be approximated by a Gaussian distribution and the rms size of this PSF is much smaller than the diffraction limit Eq. (1): $\sigma = 2.1$ um, $R = 5.6$ um.

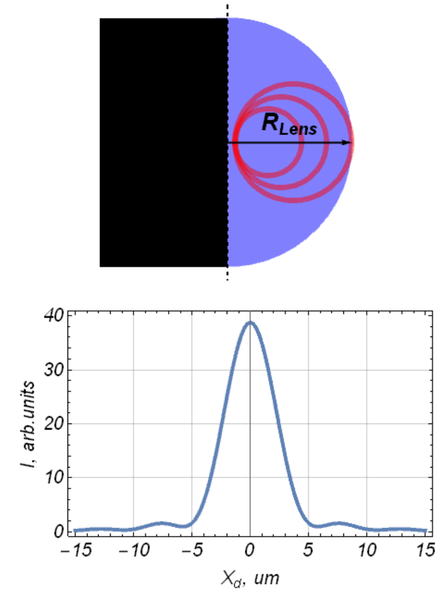

Figure 2: Scheme of the lens screening by an off-axis mask (up) and PSF distribution calculated for this case (down). Parameters: $\lambda = 0.5$ um; $\gamma = 1000$; $a = b = 500$ mm; $\theta_m = 0.1$.

The second method to improve the spatial resolution of an OTR monitor has the same purpose to create a PSF with a single maximum. Again, the OTR horizontal polarization component will be considered in the following. However, in this case the idea is to displace the imaging lens asymmetrically as depicted in Figs. 3 and 4.

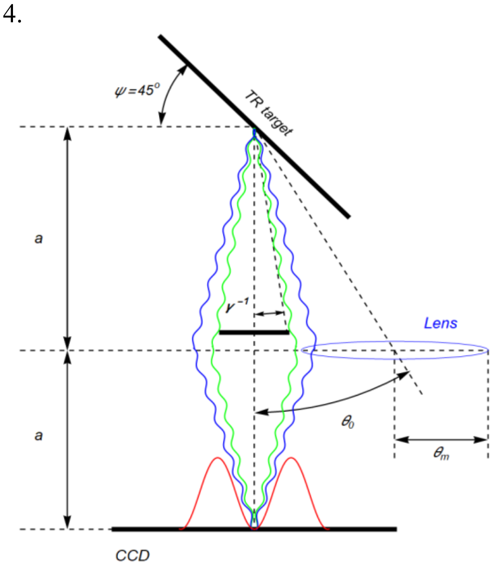

Figure 3: Scheme of the asymmetric lens displacement.

ISBN: 978-3-95450-201-1 doi:10.18429/JACoW-IBIC2018-WEPB11

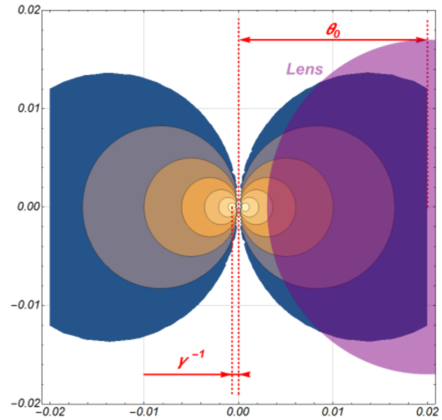

Figure 4: Scheme of the asymmetric light collection.

If the lens optical axis is disoriented with respect to the specular reflection direction from the OTR target at an angle of θ_0 with $\theta_0 - \theta_m >> \gamma^{-1}$ the OTR light will be collected from the outside region of the OTR lobe-shape distribution.

Results of such PSF calculations using asymmetric light collection geometries are presented in Fig. 5 for $\theta_m = 0.1$ rad (green points) and $\theta_m = 0.05$ rad (red points). The remaining parameters for the calculation are the same as before.

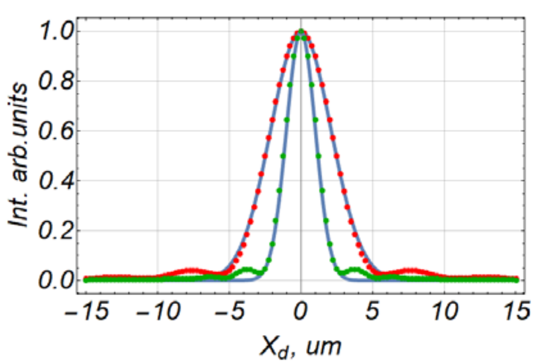

Figure 5: Calculated PSF distributions for an asymmetric lens aperture (red points $\theta_{0x} = 0.11$; $\theta_{0y} = 0$ $\theta_m = 0.05$ – red points); $\theta_{0x} = 0.11$, $\theta_m = 0.1$ (green points) and Gaussian fits for them.

Approximating the central maximum by a Gaussian distribution results in an rms value of $\sigma_1 = 1.01$ um for the first case and $\sigma_2 = 2.02$ um for the second one.

CONCLUSIONS

In the report we have showed that an off-axis mask screening of the imaging lens or an asymmetric light collection geometry caused by a displacement of the imaging lens both result in light collection from only one lobe of a linearly polarized OTR intensity distribution. As consequence, the PSF possesses also a single maximum in the image plane.

In the following PSF distributions calculated for asymmetric OTR light collection (see Fig. 2 and Fig. 5) will be compared with the well-known Airy distribution, describing the PSF of an isotropic emitting point source [9]. It is expressed as

$$AF(R_D) = (I_1(\alpha R_D)/\alpha R_D)^2, \tag{5}$$

with $I_2(x)$ the first order Bessel function and $\alpha = 2\pi\theta_m/\lambda$, $\alpha = 2\pi\theta_m/\lambda$, $R_D = \sqrt{X_D^2 + Y_D^2}$.

In Fig. 6 the Airy distribution for $\lambda = 0.5$ µm, $\theta_m = 0.1$, $Y_D = 0$ and the PSF are shown.

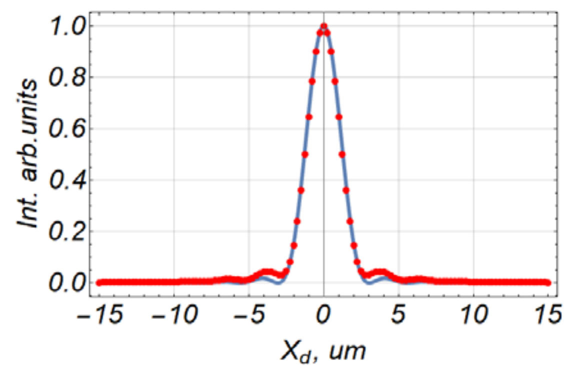

Figure 6: Airy functions for $y_d = 0$; $\lambda = 0.5$ um; $\theta_m = 0.1$ rad (blue curve) and the PSF calculated for $\theta_{0x} = 0.11$, $\theta_m = 0.1$, red dots (see Fig. 5).

One can conclude that the proposed asymmetric light collection scheme provides a spatial resolution practically coinciding with the one for an ideal isotropic source.

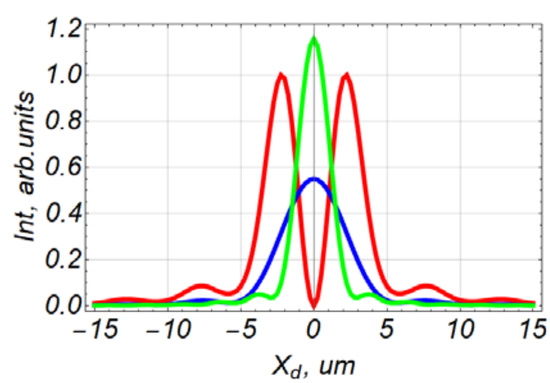

Figure 7: Comparison of calculated OTR PSF functions for conventional light collection (red line), for 50% screening of the lens aperture (blue line) and for off-axis light collection (green line)

Figure 7 compares calculated OTR PSF functions for three different cases, (i) for standard imaging without using a mask (red line), (ii) for blocking the lens aperture by an asymmetric mask (blue line), and (iii) for

Content from this work may be used under the terms of the CC BY 3.0 licence (© 2018). Any distribution of this work must maintain attribution to the author(s), title of the work, publisher, and DOI.

ISBN: 978-3-95450-201-1 doi:10.18429/JACoW-IBIC2018-WEPB11

Content from this work may be used under the terms of the CC BY 3.0 licence (© 2018). Any distribution of this work must maintain attribution to the author(s), title of the work, publisher, and DOI.

off-axis light collection (green line). All PSF functions were calculated for the same set of parameters ($\gamma = 1000$, $\lambda = 0.5$ um, $\theta_m = 0.1$). As one can see from this comparison, the PSF for the off-axis light collection has the narrowest shape and possesses only a single maximum in contrast to the PSF for standard OTR imaging which exhibits a double-lobe shape.

Drawback of asymmetric OTR observation geometries however is a decrease in the overall intensity. In the ultra-relativistic approximation (which is valid for $\gamma \geq$ 1000 with accuracy better than 1%) it is possible to estimate the OTR photon yield for the cases under consideration using the formula

$$\Delta N_{ph} = \frac{\alpha}{\pi^2}\frac{\Delta\lambda}{\lambda}\int_{\Delta\Omega}\frac{\theta_x^2+\theta_y^2}{\left(\gamma^{-2}+\theta_x^2+\theta_y^2\right)}d\theta_x d\theta_y. \qquad (6)$$

In the following the yield of the OTR horizontal polarization component is estimated (which is described by the first term in the bracket in Eq. (4)). For the screened geometry presented in Fig. 2 and an optical bandpass filter with $\Delta\lambda/\lambda = 5\,\%$ and the same aperture $(\theta_m = 0.1)$, the photon yield amounts to $\Delta N_{ph} \approx 2.4\cdot 10^{-4}\,\mathrm{ph}/e^-$. This corresponds to an intensity level of about 25% of the unpolarized OTR using a conventional imaging scheme without screening. Performing the similar calculation for the case of asymmetric light collection and a rotation of the lens optical axis at an angle of 0.11 and the same aperture, one obtains $\Delta N_{ph} \approx 1.4\cdot 10^{-4}\,\mathrm{ph}/e^-$.

We believe that the proposed technique allows to achieve a submicron resolution for a transverse beam profile diagnostics which is well above the spatial resolution of the conventional OTR monitor.

ACKNOWLEDGEMENT

The work was partly supported by the program ‘‘Nauka” of the Russian Ministry of Education and Science, grant # 3.1903.2017 and by the TPU Competitiveness Enhancement Program

REFERENCES

[1] M. Castellano and V. Verzilov, “Spatial resolution in optical transition radiation beam diagnostics”, *Phys. Rev. ST Accel. Beams*, vol. 1, p. 062801. 1998, doi: 1103/PhysRevAccelBeams.18.120198.

[2] K. Kruchinin, S. T. Boogert, P. Karataev, *et al.,* in *Proc. 2nd Int. Beam Instrumentation Conf (IBIC’13)*, 16-19 Sep., Oxford, UK, p. 615.

[3] L. G. Sukhikh, A. P. Potylitsyn, and G. Kube, “Simulation of transition radiation based beam imaging from tilted targets”, *Phys. Rev. Accel. Beams*, vol. 20, p. 032802, 2017.

[4] A. H. Lumpkin, B. X. Yang, W. J. Berg, M. White, J. W. Lewellen, and S. V. Milton, “Optical techniques for electron-beam characterizations on the APS SASE FEL project”, *Nucl. Instrum. Meth A.,* vol. 429, pp. 336-340, 1999. doi: 0.1016/S0 168-9002 (99) 00373-3.

[5] E. Chiadroni, M. Castellano, A. Cianchi, K. Honkavaara, and G. Kube,. “Effects of transverse electron beam size on transition radiation angular distribution”, *Nucl. Instrum. and Methods A,* vol. 673, pp. 56-63, 2012. doi:10.1016/j.nima.2012.01.011

[6] K. Kruchinin, A. Aryshev, P. Karataev, *et al.*, “Submicrometer transverse beam size diagnostics using optical transition radiation”, *Journal of Physics: Conference Series*, vol. 517, p .012011, 2014. doi:0.1088/1742-6596/5171/1/012011

[7] A.P. Potylitsyn, “Image of Optical Diffraction Radiation (ODR) Source and Spatial Resolution of ODR Beam Profile Monitor”, *Advanced Radiation Sources and Applications, NATO Science Series II: Mathematics, Physics and Chemistry*, Springer, N.Y., vol. 199, pp. 149–163, 2006, doi.org:10.1007/1-40203450-4_12

[8] G. Kube, “Imaging with Optical Transition Radiation, Transverse Beam Diagnostics for the XFEL”, DESY, Hamburg, Germany, Rep. TESLA-FEL 2008-01.